Berry Cactus Juice Concentrate: A Potential Modulator for Mitigating Metabolic Syndrome Markers in a High-Fat Diet Model

J. Noé García-Chavez
Instituto Potosino de Investigación Científica y Tecnológica (DMA-IPICYT)
Victoria Ramírez
Instituto Nacional de Ciencias Médicas y Nutrición Salvador Zubirán
Claudia J. Bautista
Instituto Nacional de Ciencias Médicas y Nutrición Salvador Zubirán
Mishael Sánchez-Pérez
Instituto Potosino de Investigación Científica y Tecnológica (DMA-IPICYT)
Yadira Ramírez-Rodríguez
Instituto Potosino de Investigación Científica y Tecnológica (DMA-IPICYT)
Nicolás Gómez-Hernández
Instituto Potosino de Investigación Científica y Tecnológica (DBM-IPICYT)
Robert Winkler
Center for Research and Advanced Studies of the National Polytechnic Institute
Ana K. Rocha-Viggiano
Universidad Autónoma de San Luis Potosí
Joyce Trujillo
Instituto Potosino de Investigación Científica y Tecnológica (DMA-IPICYT)
Cesaré Ovando-Vázquez
cesare.ovando@ipicyt.edu.mx

Instituto Potosino de Investigación Científica y Tecnológica (DMA-IPICYT)

Research Article

Keywords: Myrtillocactus geometrizans, metabolomic markers, Metabolic syndrome, 16S, Biomarker, Gut microbiota

Posted Date: October 16th, 2025

DOI: https://doi.org/10.21203/rs.3.rs-7688114/v1

Additional Declarations: No competing interests reported.

Abstract

Metabolic syndrome (MetS) is a multifaceted disorder influenced by genetic and environmental factors. MetS is associated with obesity, dyslipidemia, hypertension, and hyperglycemia, among others. Recently, attention has turned to gut microbiota, a diverse microbial community in the gastrointestinal tract implicated in metabolic diseases, including MetS. Berry cactus (*Myrtillocactus geometrizans*) contains polyphenols, pectins, sterols, and betalains with hypoglycemic, hypolipemic, anti-inflammatory, and antiproliferative properties. This study investigates the impact of berry cactus juice concentrate (BJC) consumption on gut microbiota diversity and its modulation in a rat model of MetS development by a high-fat diet. Metabolic markers related to MetS and comprehensive analyses of microbial 16S rRNA gene were obtained after 140 days of treatment. Correlations between metabolic parameters, relevant microbial genera, and predicted functions and pathways were linked to MetS. BJC administration diminished the serum levels of fasting blood glucose, triglycerides, total cholesterol, leptin, insulin, and ileal fat percentage. Furthermore, BJC treatment was associated with alterations in the composition of the gut microbiota, favoring microbial phyla associated with metabolic health. Specifically, an association with the *Parabacteroides* genus was observed, suggesting potential mechanisms of action, including modulation of cellular pathways involved in fatty acid metabolism and promotion of the availability of berry cactus bioactive molecules. These findings highlight the potential of BJC consumption as a promising therapeutic approach for individuals with MetS or those at risk of its development, offering insights into the intricate interplay between dietary patterns, gut microbiota, and metabolic health.

1. Introduction

Metabolic syndrome (MetS) is a multifactorial disease caused by a complex interaction of genetic and environmental factors, it is characterized by a cluster of metabolic abnormalities, including abdominal obesity, insulin resistance, hyperglycemia, dyslipidemia, hypertension, oxidative stress, pro-inflammatory and prothrombotic processes, endothelial and adipose tissue dysfunction, and abnormalities in metabolic and cellular pathways, which collectively increase the risk of type 2 diabetes and cardiovascular disease [1]. MetS prevalence has risen globally, with reported rates of 35 % n the United States [2], 40 % in he Middle East [3], and 41 % in Mexco [4]. Given its growing global public health impact, novel interventions targeting its underlying mechanisms are essential. Gut microbiota, which plays a crucial role, is a key emerging factor in MetS physiopathology. The main commensal microbial phyla are *Proteobacteria*, *Actinobacteria*, *Verrucomicrobia*, *Firmicutes*, and *Bacteroidota*, with the latter being the most predominant in the gastrointestinal tract. Dysbiosis can lead to allergies, inflammatory bowel disease, non-alcoholic fatty liver disease, obesity, and MetS [5]. Gut microbiota exerts a direct systemic influence on its host, making it a crucial indicator of the host´s metabolic status. The complexity of gut microbiota is challenging; however, recurring patterns of microbial composition have been grouped into clusters termed “enterotype” [6]. These enterotypes are established using different metrics, including alpha species diversity, the ratio of *Firmicutes* to *Bacteroidetes* phyla, or the relative abundance of beneficial genera (e.g., *Bifidobacterium* and *Akkermansia*) versus facultative anaerobes

(*Escherichia coli*), pro-inflammatory (*Ruminococcus*), or nonbacterial microbes (*Saccharomyces*) [6]. The presence of different phyla has been correlated with physiological parameters such as age, sex, and body mass index, and is associated with several diseases [6], altering multiple signaling pathways that still require further research for a full understanding.

Dietary compounds are mainly metabolized by microbiota, producing functional metabolites that impact human metabolism and health while promoting specific gut diversity. For example, short-chain fatty acids, trimethylamine N-oxide, and lipopolysaccharides may affect the heart, gut, liver, kidney, and adipose tissues, among others [7]. *Myrtillocactus geometrizans*, a mexican endemic cactus with edible fruit commonly known as “garambullo” or berry cactus, contains bioactive compounds in the fruit, mainly metabolites such as polyphenols, pectins, sterols, and betalains (betacyanins and betaxanthins) and phenolic compounds, which exhibit antibacterial, hypoglycemic, hypolipemic, antioxidant, anti-inflammatory, and antiproliferative properties [8]. To the best of current knowledge, no studies have been conducted on the effect of berry cactus administration on MetS. In this regard, it has been reported that polyphenolic and flavonoid metabolites contained in the berry cactus have beneficial effects on weight reduction associated with a reduction in food consumption, favoring weight loss by proper energy metabolism and limited oxidative stress [8]. Additionally, the metabolism of phytochemicals in the host is significantly influenced by microbiota via bacterial enzymes (e.g., α-L-rhamnosidase, dioxygenases, and bile salt hydrolases) [9], which may beneficially impact intestinal and systemic health through by-products formed during the colonic metabolism of the non-digestible fraction of the berry cactus [10].

This study focuses on microbiota diversity and its modulation by berry cactus consumption in the context of MetS, an emerging and significant research area. This study aimed to identify microbial biomarkers associated with MetS and berry cactus consumption through comprehensive analyses of 16S amplicon data and to identify associations between metabolic markers and the abundances of MetS-associated genera.

2. Material and Methods

2.1 Obtaining fruit and berry cactus juice concentrate (BJC)

Fruits were collected between June and July 2021 at La Labor del Río, San Luis Potosí (21º46'46" N 100°36'37" O). Fresh berry cactus juice was extracted as previously reported for similar cactus fruit [11]. The BJC supernatant underwent a proximal analysis before being stored in aliquots at 80°C. Aliquots were lyophilized (277.12g) at 63°C under 3 Pa for 48 h and protected from light at 20°C until use.

2.2 Chemical approximate analyses of the BJC

The chemical analysis of the BJC composition was performed by the Centro de Investigación y Asistencia en Tecnología y Diseño del Estado de Jalisco A.C. using Mexican Official Standards based on AOAC methods (Official methods of analysis of AOAC International) [11]. The mass (g/100 g) of the sample was determined using the moisture (%) obtained by BJC evaporation from a heat treatment

using the following equation: moisture (%) = [(wet sample weight dry sample weight)/sample weight 100]. Ash is the dry residue obtained by incinerating and calcining the BJC sample at 600°C and quantification of total ash. Crude fiber was digested with sulfuric acid (BJC), and the insoluble residue of crude fiber and salts was filtered, dried, weighed, and calcined for weighing again. These analyses were performed gravimetrically. The Soxhlet method was used to determine the fat content. Briefly, the fat content in 2 g of BJC was determined by acid hydrolysis of the protein-fat complex (33% hydrochloric acid). Subsequently, the fat was extracted with petroleum ether at 30°C–60°C using a Soxhlet extractor, and the fat was quantified directly. The protein content was measured using the Kjeldahl method, and the total carbohydrates were determined by the difference of proximal analysis using the following equation: total carbohydrates (%) = [100 (protein + lipids + ash + crude fiber)]. All samples were expressed as g/100 g and analyzed from at least two independent experiments. Supplementary Table 1A shows the results.

2.3 Guide and experimental model handling and maintenance

Experiments were performed with the approval of the Care Committee and Use of Animals of the Medicine Faculty of the Universidad Autónoma de San Luis Potosí (BGFM UASLP-22-24) according to the ARRIVE 2.0 Guidelines and the National Institutes of Health. The animals were housed in individual cages and maintained in a controlled temperature room (20–22°C), humidity (44–66%), and illumination (12-h light/dark cycle) throughout the research protocol. The animals were fed a standard diet and water *ad libitum* at the beginning of the research protocol and acclimatized for one week.

2.4 Experimental protocol

Twenty male Wistar rats (120–150 g, 21 days old) were randomly divided into four groups (n = 5) Fig. 1: the control group receiving AIN-93 diet plus 1 mL of sterile water (control); the second group received AIN-93 diet plus 200 mg/kg of BJC lyophilized and hydrated with 1 mL of sterile water (BJC); the third group received a high-fat diet (HFD) based on AIN-93 with 45% calories from lipids based on lard [12] plus 1 mL of sterile water; and the fourth group was treated with HFD plus 200 mg/kg of BJC lyophilized and hydrated with 1 mL of sterile water (HFD + BJC). The AIN 93 diet was paired with the average weekly HFD consumption; the animals that received AIN 93 were supplemented with drinking water, while the HFD groups were supplemented with 2.5 % scrose in drinking water *ad libitum* during the 20 weeks of dietary regimen. The BJC dose was established based on our group's studies using a pitaya juice concentrate derived from cactus fruit (*Stenocereus huastecorum*), which has a similar chemical composition and bioactive metabolites [13]. All sterile water and BJC treatments were dispensed daily by gavage (G18), following reported protocols [11], for 140 days. Body weight and food and water intake were recorded daily. Subsequently, the animals were euthanized after anesthesia with sodium pentobarbital from PISA (Guadalajara, Jalisco, México; 90 mg/kg, i.p.), and blood was collected from the aorta in heparinized tubes (50 U/mL). The samples were centrifuged at 1,470 g at 4°C for 10 min, and the plasma was collected and stored at − 20°C for determination of biochemical parameters. Subcutaneous adipose tissue, right inferior lobule of the liver, and intestine (ileum and jejunum regions) were collected

to assess the total fat percentage following the modified Folch method [11]. Fresh fecal samples from rats were collected in sterile tubes 48 h before sacrifice and were stored at 80°C until further analysis.

The clinical criteria for MetS diagnosis in diet-induced rat models were established according to previous studies in rodents and humans, which include an increase of 3 or more clinical parameters as follows: increase in body weight, high body mass index, hyperglycemia, insulin resistance, triglycerides, total cholesterol (TC), decrease in high-density lipoprotein cholesterol (HDL-C), and increase in diastolic and systolic blood pressure. After 140 days of treatment, the following criteria were met: body weight ≥ 432 g, fasting plasma glucose ≥ 151 mg/dL, triglycerides ≥ 109 mg/dL, TC ≥ 121 mg/dL, and an increase in total fat mass (subcutaneous and visceral) of ≥ 20%.

2.3.1 Diets

The control diet was formulated to mimic the typical proximate composition of the AIN-93G diet for rodent growth, pregnancy, and lactational phases, with minor adjustments. For the HFD, two variables were incorporated: fat content (45%, plus 2.5% of sucrose in the drinking water) and the addition of BJC (200 mg/kg; HFD + BJC). Both diets were prepared as previously described by Avila-Nava *et al.* (2017) [12]. Supplementary Table 1B shows the formulations. Cornstarch, Casein (85 % potein), maltodextrin, cellulose, and Tert-butylhydroquinone were purchased from Ingredion (Westchester, IL, USA) in Ampher Foods (CDMX, México). Mineral and Vitamin mix were purchased from MP Biomedicals (Santa Ana, CA, USA). L-Cystine and choline bitartrate (41.1% choline) were purchased from Sigma-Aldrich (St. Louis, MO, USA). Sucrose, soybean oil, and lard were purchased from HEB (San Antonio, TX, USA). All reagents used were of feed grade.

4. Biochemical analysis

According to our previous reports [11], the levels of glucose, triglycerides, TC, ALT, AST, creatinine, and blood urea nitrogen (BUN) were determined to assess metabolic changes in plasma using spectrophotometry with commercial kits (Spinreact; Girona, Spain). Serum insulin and leptin levels were determined using ELISA assays with commercial kits following the manufacturer's instructions (Merck & Co., Inc; Rahway, NJ, USA).

5. Collecting fecal samples and obtaining DNA from rat feces

Microbial DNA content was extracted from fecal samples using a commercial kit (Zymo Research, Orange, CA, USA) following the manufacturer's instructions. DNA was quantified and stored frozen at −80°C.

6. Fecal community 16S gene analysis

Microbial DNA was amplified by polymerase chain reaction (PCR) using the 16S rRNA forward primer: 5´TCGTCGGCAGCGTCAGATGTGTATAAGAGACAGCCTACGGGNG3´ and the reverse primer: 5´GTCTCGTGGGCTCGGAGATGTGTATAAGAGACAGGACTACHVGGGT3´.

The PCR was performed under the following conditions: preheating at 94°C for 4 min, followed by 25 cycles of denaturing at 94°C for 30 s, annealing at 56°C for 30 s, elongation at 72°C for 45 s, and finally a single step of 72°C for 7 min. The samples were pooled and sequenced in a 2x300 paired-end format with the Illumina MiSeq platform (MiSeq Reagent Kit V.3, 600 cycles, San Diego, CA, USA) according to Illumina's protocol (16S metagenomic sequencing library preparation).

7. 16S amplicon sequencing

The 16S sequencing data were processed using the DADA2 v1.16.0 R package. The filterAndTrim() function was used with default parameters to trim 20 at to the right of the forward fragments and 60 at to the right of the reverse fragments. The default settings of the *learnErrors*() function were used to determine the error rates. The filtered fragments computed error rates, and default settings of the *dada*() method were used to deduce the sample composition. The *mergePairs*() method was used to combine fragments with a minimum overlap = 10 and maximum mismatches = 2, and the *removeBimeraDenovo*() function with default parameters was employed to eliminate chimeras. The taxonomy for each sequence was determined using the silva_nr99_v138 database and the assignTaxonomy() method. The ASV quantification and their phylogenetic assignment were obtained from these results.

The diversity() function of the vegan v2.5.6 R package was used to calculate the alpha diversity, Shannon, inverse of Simpson, Fisher, Chao1, and abundance-based coverage estimator (ACE) indices. Plots of beta diversity and NMDs were created using custom R scripts to ascertain the structural variation of microbial communities, and the BrayCurtis dissimilarity was computed using the *ordinate*() function from the vegan package.

The 16S sequencing data were functionally predicted using Tax4Fun2. The runRefBlast() and makeFunctionalPrediction() functions were utilized with default parameters to forecast the functional profiles of the ASV quantification results. RF99NR was the reference used in the runRefBlast and makeFunctionalPrediction stages. The abundance and pathway data were used in the sparse partial least squares discriminant analysis (sPLS-DA) permutation test. The spls-da() function of the R package MixOmics was employed, with ncomp = 2 and default parameters. The graphs representing the findings of the DA were created with custom R scripts.

Taxa-pathway networks (permutation test sPLS-DA, 1,000 permutations, p-value < 0.1) were constructed using relevant taxa and routes. The igraph Rpackage uses the Spearman correlation between two nodes (taxa or routes) to determine their relationship. Only correlations with a p-value < 0.05 and False Discovery Rate (FDR) < 0.1 were considered for building the networks.

8. Association between biochemical and 16S data

Correlation of biochemical parameters with genus abundances, pathways, and functions was performed using the Spearman rank correlation test from the R stats package.

9. Genomic analysis of taxonomic groups associated with biochemical parameters

Three main groups of pathways associated with the biochemical parameters were identified. The genomes of several species of relevant genera were annotated to confirm the presence of genes in the pathways in each group. The genomes used in this study were retrieved from the National Center for Biotechnology Information database. Quality checks were performed to ensure genome completeness and sequencing coverage. Genomes were selected from three distinct groups: group 1, *Parabacteroides* and *Bacteroides*; group 2: *Akkermansia, Candidatus Saccharimonas, Adlercreutzia*, and *Clostridium sensu stricto*; group 3: *Allobaculum, Clostridium sensu stricto 1, Adlercreutzia, Faecalibacterium, Intestinimonas, Ligilactobacillus*, and *Turicibacter.* Genomes of these genera were used for gene prediction and comparative analyses within each taxonomic group. Genomes were annotated using Prokka to standardize gene annotation and gather genetic information. Predicted proteins from annotated genomes were functionally annotated using the Eggnog database to elucidate biological functions and infer functional relationships. The Kyoto Encyclopedia of Genes and Genomes (KEGG) orthology matched groups of corresponding genes with annotated pathways.

10. Statistical analysis

Biochemical parameters are expressed as mean ± standard deviation. Kolmogorov-Smirnov tests were performed to determine whether the data were normally distributed. Two-sided Student’s t-tests were performed, and when data were non-normal, Welch’s t-tests were performed to identify significant differences in the biochemical parameters assessed.

3. Results and discussion

3.1 Administration of BJC significantly improved the outcome of HFD-induced MetS in rats

Unhealthy eating habits and a sedentary lifestyle are major risk factors for obesity and metabolic syndrome. Lifestyle interventions often provide pharmacological and surgical treatment with adjuvant results. Thus, addressing these habits, primarily through diet, is essential for managing progressive MetS [14]. In this study, the effects of BJC on diet-induced MetS in rats were investigated. At the beginning of the experiments, no significant differences in body weight, glucose, triglycerides, TC, ALT, and AST were observed between groups. However, after 140 days, the rats fed with HFD exhibited a marked increase in

body weight compared with those on an AIN-93 diet (679 ± 110.63 g *vs* 434.8 ± 16.39 g, *p*-val. = 2.18E-05), indicating that the HFD induced overweight (Table 1). The BJC treatment significantly reduced body weight gain in the HFD + BJC group (611 g ± 46.82) compared to the HFD group (679 g ± 110.62). The control and BJC groups showed a similar weight gain among themselves (434.8 g ± 16.39 and 440 g ± 36.69, respectively).

Table 1
Biochemical parameters evaluated.

Biochemical parameter	Control	BJC	HFD	HFD + BJC	HFD vs Control *p*-val.	HFD + BJC vs Control *p*-val.	HFD + BJC vs HFD p val.	HFD + BJC vs BJC p val.
Weight (g)	434.80 ± 16.39	440 ± 36.69	**679 ± 110.63**	**611 ± 46.82**	**2.18E-05**	**0.0005**	0.25	**0.0002**
ALT (U/L)	15.05 ± 5.13	11.20 ± 2.52	12.83 ± 5.58	10.38 ± 3.48	0.45	0.13	0.43	0.68
AST (U/L)	37.10 ± 8.93	29.05 ± 11.12	36.64 ± 19.21	26.25 ± 6.79	0.77	0.064	0.30	0.64
Creatinine (mg/mL)	0.51 ± 0.19	0.69 ± 0.11	**0.83 ± 0.05**	0.84 ± 0.17	**0.0038**	**0.017**	0.9	0.15
BUN (mg/mL)	19.18 ± 2.54	24.88 ± 3.15	28.19 ± 2.72	**21.79 ± 5.41**	0.21	0.36	**0.06**	0.32
Total hepatic fat (%)	3.16 ± 0.93	3.33 ± 0.64	**5.94 ± 1.72**	5.25 ± 0.61	**0.0004**	**0.005**	0.44	**0.013**
Total intestinal fat (jejunum) (%)	11.24 ± 3.94	13.89 ± 6.75	**23.01 ± 4.35**	23.88 ± 5.54	**0.0009**	**0.018**	0.81	**0.072**
Total intestinal fat % (Ileum) (%)	14.26 ± 13.41	14.65 ± 15.05	**6.08 ± 2.94**	3.66 ± 1.30	**0.051**	0.14	0.19	0.17
Total adipose tissue fat (%)	5.84 ± 1.40	8.86 ± 2.53	12.32 ± 3.56	9.85 ± 2.12	0.56	0.022	0.23	0.68

[a] The mean and standard deviation of each parameter are shown. Control, AIN-93 diet control group. BJC, Berry cactus juice concentrated (200mg/kg), AIN-93 diet plus BJC treatment group. HFD, high-fat diet group (45%). HFD-BJC, high-fat diet with berry cactus treatment. Significant differences in biochemical parameters are marked with *, p-val. < 0.05 (Welch's T test).

Evidencing the impact of an HFD on metabolic health by significant weight gain and metabolic disturbances, including hyperglycemia, hypertriglyceridemia, hypercholesterolemia, hyperleptinemia, and hyperinsulinemia, which are hallmarks of MetS and align with the guidelines of the National Endocrinology Program ATP-III, the World Health Organization, and the International Diabetes Federation for MetS diagnosis [14]. In this study, HFD group exhibited a significant increase in metabolic markers compared to control group, they presented a hyperglycemia (Δ 62 mg/dL, *p*-val. = 0.00009), hypertriglyceridemia (Δ 48.25 mg/dL, *p*-val = 0.001), hypercholesterolemia (Δ 30.59 mg/dL, *p*-val. = 0.013), hyperleptinemia (Δ 117.34 pg/mL, *p*-val. = 0.014), and hyperinsulinemia (Δ 10.59, *p*-val. = 0.002), as shown in Fig. 2a-e, respectively. This group also showed increased serum creatinine concentration (Δ 0.24 mg/mL, *p*-val. = 0.003 (Table 1). In addition to increasing the total hepatic fat percentage (Δ 2.4 %, -val. = 0.0004), and the total jejunum fat percentage (Δ 11.01 %, -val. = 0.0009) and decreased compared with the total ileum fat percentage (Δ 9.64 %, -val. = 0.051) with the control group (Table 1). In response to a substantial fat load, elevated serum creatinine levels, along with increased hepatic and jejune fat percentages in the HFD group, provide additional evidence of metabolic dysfunction, confirming the detrimental effects on health, pointing out the importance of the liver and intestine in the body's adaptation to the metabolic changes induced by HFD exposure [15].

In contrast, the HFD + BJC group exhibited a significant reduction in serum TC (Δ -37.16 mg/dL, *p*-val. = 0.06), insulin (Δ -8.25 ng/mL, *p*-val. = 0.1), and BUN levels (Δ -6.4 mg/mL, *p*-val. = 0.06) compared with the HFD group, as shown in Fig. 2c, e, and f, respectively. There was also a decrease in fasting blood glucose (Δ -18.9 mg/dL, *p*-val. = 0.2), triglycerides (Δ -13.8 mg/dL, *p*-val. = 0.48), and leptin levels (Δ -86.89 pg/mL, *p*-val. = 0.27) (Fig. 2a, b, and d). In addition to total hepatic fat, intestinal fat (jejunum), and adipose tissue fat, these changes did not reach statistical significance (Table 1). Furthermore, there were no significant differences in ALT and AST levels between the groups (*p*-val. = 0.3 and 0.43, respectively).

These findings suggest that BJC supplementation mitigates some of the metabolic alterations induced by HFD, particularly by improving lipid and glucose metabolism (significantly reducing serum TC, insulin, and BUN levels) and reducing total fat accumulation in the ileum. No significant effects on glucose, triglycerides, leptin, ALT, and AST levels, nor on total fat accumulation in the liver, jejunum, and adipose tissue (Table 1). Previous studies with a similar model (49% lard) showed that administering a leaf extract from *Cecropia peltata* for 90 days significantly reduced serum glucose and lipid levels [16]. Note that the follow-up period in the present study was 140 days and 45%-lard, which may be related to the differences between previous studies (AIN93 diet-based). In this study, the benefits of cactus fruit-based interventions in promoting weight loss, associated with minor total adipose and ileum fat percentage, and normo insulinemia, which have the potential to improve overall health outcomes, considering the strong link between MetS and various diseases.

In addition, in this study investigated the liver and kidneys, which play a critical role in glucose metabolism. High serum TC, insulin, creatinine, and BUN levels confirmed that HFD intervention disrupted liver and kidney function. Notably, treatment with BJC effectively decreased serum insulin,

leptin, creatinine, and BUN levels without modulating liver enzymes (ALT and AST), providing evidence of BJC´s ability to regulate liver and kidney function. In this regard, an experiment made with streptozotocin-induced diabetic rats that received 4 g/kg berry cactus juice showed diminished circulating glucose, TG, and TC levels, in addition to improved renal function. It was associated with the re-establishment of glutathione and glutathione S-transferase levels in renal tissue, compared to non-treated diabetic rats. This report concluded that the renoprotective properties can be attributed to dietary bioactive compounds, including flavonoids, phytosterols, phenolic acids, betalains, and antioxidants [15].

3.3 BJC administration significantly alleviated HFD-induced gut dysbiosis in the MetS experimental model

In last decade, microbiota has emerged as a new factor associated with MetS pathophysiology [5]. Dysbiosis contributes to MetS development, but its molecular mechanisms remain poorly understood [5]. The critical commensal microbial phyla include *Proteobacteria*, *Actinobacteria*, *Verrucomicrobia*, *Firmicutes*, and *Bacteroidota*, with the latter being the most dominant in the gastrointestinal tract [5]. To investigate the impact of BJC intervention on the abundance of specific bacterial taxa, a 16S analysis of community composition at the phylum level was conducted. On average, ~ 10,000 fragments were sequenced per sample, with five replicates per group. The total abundance per group showed no differences, except for HFD + BJC_rep1 (almost 60,000 fragments) and HFD + BJC_rep20 (less than 1000 fragments; Supplementary Fig. 1), which were excluded.

In Fig. 3a shows that the control group showed *Firmicutes* and *Bacteroidota* as the most abundant (~ 53% and 38%, respectively), followed by 3.5% *Campylobacterotaby, Patescibacteria*, and *Proteobacteria* (~ 2%, respectively) and 0.01% *Verrucomicrobiota.* The BJC group showed 43.1% *Firmicutes* and ~ 51% for *Bacteriodota*, 3% *Verrucomicrobiota*, 2.1% *Proteobacteria*, while < 1% *Patescibacteria*. While, HFD group had ~ 54% *Bacteroidota*, ~ 41% *Firmicutes*, 0.06% *Proteobacteria*, ~ 2% *Patescibacteria, and Campylobacterotaby.* The < 1% *Verrucomicrobiota*. The administration of BJC in rats with HFD (HFD + BJC) induced an increase in *Firmicutes* to ~ 64%, and a reduction in *Bacteroidota* to 18%. *Proteobacteria, Actinobacteriota, and Verrucomicrobiota increased* to 11%, 3.5%, and 1.1%, respectively. BJC induce a diversity restoration of *Firmicutes* and *Proteobacteria* in this model, which were decreased in the HFD group. So, *Firmicutes* and *Bacteriodota* were the most abundant phyla in all groups. However, their abundance differs across the groups. According to the present findings, HFD increased the abundance of the *Parabacteriodes* genus, and BJC reversed those changes. This result is like those observed by other groups, where its increase was associated with metabolic imbalance, an increase in body weight, and in lipid metabolism, including TC and TGs, among others [17]. In fact, it was described that the presence of *Bacteroidetes* strain was associated with increased *B. fragilis* and *P. diastolic*. The reduction in the metabolism of carbohydrates and decrease short-chain fatty acids in the gut have been related to MetS development, as we can see here, BJC addition restores the diversity; this effect was also seen in MetS patients that were fed with a Mediterranean diet with high concentrations of polyphenolic compounds, increase the abundance of beneficial bacteria like *Enterococcus*, *Prevotella*, and

Bacteriodetes [18]. Phylum relative abundance in each of the replicates of all groups is shown in Supplementary Fig. 2.

These results shown that the Alpha diversity was higher in the HFD + BJC group, showing higher Shannon and Simpson's diversity compared with the other groups (4.885 and 0.984, respectively; Fig. 3b, cyan boxes). The Shannon diversity mean was 4.04, 4.19, and 4.15 (Fig. 3b, right panel), and the Simpson's diversity mean was 0.975, 0.977, and 0.973 (Fig. 3b, left panel) for the control, BJC, and HFD, respectively. Supplementary Table 2 presents the alpha diversity values of all the groups. Meanwhile, beta diversity analysis showed that HFD + BJC has higher similarity to the control than to the HFD group (Fig. 3c), likely due to gut microbiota disruption dominated by *Bacteroidetes* and *Firmicutes*.

Besides, a sparse partial least-squares Discriminant Analysis (sPLS – DA) permutation test was used to identify relevant taxa between groups. Initially, there was no clear group differentiation in the clustering pattern, including all genera (Fig. 4a). After sPLS-DA considering only the variables with significant changes for each group, a clear differentiation was observed in the clustering pattern (Fig. 4b), identifying relevant genera surrounded by HFD *versus* HFD + BJC, as shown in Fig. 4c and Fig. 5.

Specifically, Fig. 5a shows that the control, BJC, and HFD groups had similar abundances of *Parabacteriodes*, but it was significantly reduced in the HFD + BJC group. Further analysis revealed that the HFD + BJC group reduced the *Helicobacter* genus relative to the control and HFD groups. In addition, it was observed that only BJC administration reduced the abundance of the *Helicobacter* taxa in both the control and HFD groups. Thus, BJC directly modulates *Helicobacter* genus reduction, independent of diet composition (Fig. 5b). Similar results were observed by Jin & Zhang (2020), who reported a reduction in *Helicobacter*, which was associated with a pro-inflammatory gut environment and an increase in carcinogenesis in animals fed with HFD [19]. *H. pyllori* infection has been associated with insulin resistance, lipotoxicity and liver damage. Interestingly, red wine or grape juice consumption has been associated with reduced *Helicobacter pylori* symptoms [20]. Here, it was observed that BJC reduces the *Helicobacter* genus, so BJC may help to minimize dysbiosis due to similarities between the compositions of juices.

A few genera were present in only one group, *e.g.* the *Weissella* genus was present in low abundance in the HFD group (Fig. 5c) and the *unclassified NK4A214* group, which was present in BCJ-treated rats (Fig. 5d). In particularly, the low abundance of *Weissella* genus has been previously described and has been associated with reduced dysbiosis in the MetS model. In this respect, *Weissella cibaria MG5285* has been related to the reduction of metabolic parameters such as glucose and lipogenic proteins like fatty acid synthase, peroxisome proliferator-activated receptor gamma, and sterol regulatory element-binding protein 1c, inflammatory marker reduction, and an increase in bacteria strains that increased short-chain fatty acid production. This effect was proved in a mouse model showing the same effects and an increase in insulin secretion and reduction of fat mass [21]. Thus, the lower abundance of the *Weissella* genus in the HFD group may mediate a beneficial effect on rats in the present study. However,

this genus has also been associated with the harmful impacts of having a dual function. Some strains have been reported to have pathogenic potential.

Additionally, the genus *Lactobacillus* did not show substantial changes between the control, BJC, and HFD groups, whereas it showed increased abundance in the HFD + BJC groups (Fig. 5e). *Lactobacillus* abundance has been linked to lower body weight, glucose, and insulin levels, and improves lipid metabolism [22]. The increase in the treated group (HFD + BJC) may indicate an improvement in lipid metabolism, which correlates with the biochemical parameters.

In the case of *Faecalibaculum* and *Bifidobacterium*, the abundance was only present in the HFD + BJC group (Fig. 5f and g, respectively). In this regard, an increase in the abundance of several short-chain fatty acid-producing bacteria, such as *Faecalibaculum rodentium* and *Bifidobacterium*, has been reported in mice fed an obesogenic diet co-supplemented with cranberry polyphenol extract [23], among others. In this study, an increase in *Bifidobacteria* in the HFD + BJC group was associated with reduced metabolic markers, lipids, leptin, and insulin levels, promoting an anti-obesogenic environment [24]. Berry juices have been linked to increased *Bifidobacterium* abundance, which exhibits anti-inflammatory and cardioprotective effects [25].

Whereas the abundance of *HT002 (Limosilactobacillus)* was significantly higher in the HFD + BJC group than in the other groups (Fig. 5h). BJC administration in HFD-fed animals showed significant presence of *Desulfovibrio, Adlercreutzia*, and *C. sensu stricto 1* (Figs. 5i, j, and l, respectively). In addition, BJC supplementation showed a relative abundance of *Desulfovibrio* and *Clostridium sensu stricto 1* when compared with other groups in the study. The increase in these two taxes is usually related to pro-inflammatory effects and endotoxemia [26]. In this regard, Jiao *et al*. (2019) suggested that blueberry polyphenol extract, as a potential prebiotic agent, influences the gut microbiota to positively affect HFD-induced obesity in C57BL/6J mice, highlighting a significant increase in abundance in *Desulfovibrio*, *Adlercreutzia*, and *Bifidobacterium*, which is associated with improved glucose tolerance [27].

In the case of *Akkermansia* taxa, no changes were observed between the control and HFD groups; however, BJC consumption increased significantly regardless of the dietary pattern (Fig. 5k). Similar results have been reported using a polyphenol-rich cranberry extract in C57BL/6J mice treated with MetS (200 mg/kg/day for 8 weeks) and in healthy humans treated with Prebiocran™ for 4 days [28], showing a proportional abundance increase in *Akkermansia* spp. These changes were associated with beneficial metabolic effects and anti-obesogenic effects, respectively, through reduced weight gain, visceral obesity, improved insulin sensitivity, decreased liver weight, attenuated serum levels of AST and ALT [28], and triglyceride accumulation associated with blunted hepatic oxidative stress and inflammation. Notably, the metabolic effects observed in the mentioned study are similar to those observed in animals with MetS supplemented with BJC.

Fusicatenibacter, Phascolarctobacterium, and *Incertae sedis* did not show any changes (Fig. 5m, n, and p). Considering all reports and the results in this study, the lack of changes may reflect interindividual variability linked to specific gut microbial ecologies and bioactive diets, such as those including

polyphenols, which are associated with the dietary patterns and probably with the content of bioactive compounds content of BJC [29].

The *Caproiciproducens* genus showed a significant increase in BJC rats compared with the HFD + BJC group (Fig. 5o), without observing substantial changes in the HFD group. *Caproiciproducens* is an anaerobic bacterial genus that produces medium-chain fatty acids, particularly caproic acid. Its presence has been associated with fermentative metabolism, lipid metabolism, and gut barrier function. It has been observed that the administration of 200 mg/kg of wild blueberry polyphenol extract in high-fat, high-sucrose-fed C57BL/6J male mice for 8 weeks resulted in a tendency toward a greater abundance of several fermenting genera, including *Caproiciproducens* [30], associated with improved glucose tolerance and restored intestinal mucus integrity [31].

The *Lachnospirceae UGC-008* genus shows a reduction in HFD rats compared with the control group animals, although this difference is not significant. The BJC consumption in rats with HFD significantly increased the presence of this genus, as shown in Fig. 5q. Finally, *C. Saccharimonas* was abundant in the HFD group, and BJC supplementation potentiated its abundance compared with the BJC group (Fig. 5r). These results align with previous reports showing that in obese Spanish [32] subjects, the abundance of the *Lachnospiraceae* genus was significantly lower in obese compared with lean subjects, and the abundance of gut microbiota was directly related to body mass index. Furthermore, Sprague-Dawley rats fed a 45% HFD for 81 days showed a significant increase in *C. Saccharimonas* from the first week of HFD feeding, which became more pronounced after 11 weeks [33], like our case.

Overall, the findings to this point suggests that BJC improves metabolic markers, including less accumulation of body fat in tissues, reductions in serum TC, TG, leptin, and insulin levels, while persevering microbiota diversity in MetS rats, potentially through its dietary bioactive compounds (polyphenols, pectins, and sterols) [15], which might stimulate the proliferation of beneficial bacteria [10] or limit MetS-related phyla to restore the abundance and uniformity of the HFD-induced microbial community to levels similar to the control group. The enhanced alpha diversity, shown as a higher Shannon and Simpson's diversities in the HFD + BJC group, further reinforces this protective effect, as greater microbial diversity has been linked to better metabolic health [6, 7]. Nevertheless, this study has some limitations that need to be addressed. Further investigation is required to confirm the changes in the microbiome caused by BJC in the human MetS population.

1. **BJC significantly modulates microbial metabolic pathways and health-promoting functions and is associated with microbiome abundance shifts in a MetS model**

The abundances of various genera and cellular pathways were further analyzed to explore the role of the bacterial microbiota in MetS. Using sPLS-DA, specific pathways associated with different treatments were identified. This pathway analysis offered further insights into the molecular mechanisms underlying the observed changes. Here, enriched functions, signaling, and metabolic pathways are described, with only correlations having a p-value < 0.1 being described. The complete association network between genus abundance and pathways is shown in Fig. 6 and Supplementary Fig. 3.

First, the nodes of relevant taxa (yellow circles) and pathways (green squares) of HFD (blue color) and HFD + BJC (red color) groups are highlighted. In Fig. 6, only relevant pathways for HFD + BJC were base excision repair, starch and sucrose metabolism, glucagon signaling pathway, RNA polymerase, glycolipid metabolism, and tropane, piperidine, and pyridine alkaloid biosynthesis pathways, suggesting that BJC modulates these pathways to restore metabolic balance in MetS. Specifically, in relation to glycolipid metabolism, which correlated positively with beneficial genera such as *Lactobacillus*, *Faecalibaculum*, and *Bifidobacterium*, previous studies have demonstrated that these strains play an essential roles in carbohydrate fermentation, gut permeability, and inflammation [5].

Moreover, seleno-compound metabolism, degradation of aromatic compounds, platinum drug resistance, cysteine and methionine metabolism, and benzoate degradation were also relevant for HFD + BJC compared to HFD (Fig. 6) and control (Suppl. Figure 3). Meanwhile, sphingolipid metabolism, glyoxylate and dicarboxylate metabolism, other glycan degradation, and peroxisome pathways were relevant for all experimental groups compared to HFD + BJC. This suggests that the microbiota becomes enriched in these pathways following BJC administration in the context of HFD.

Furthermore, Fig. 6 shows that in the HFD and HFD + BJC comparison, a positive correlation (red line) was found between the genera UCG-005 and *NK4A214, Lactobacillus*, *HT002*, *Adlercreutzia*, *Faecalibaculum*, and *Bifidobacterium*. These genera were positively correlated with glycerolipid metabolism, benzoate degradation, and biosynthesis of tropane, piperidine, and pyridine alkaloids. Furthermore, *Lactobacillus* was negatively correlated (blue line) with *Helicobacter* and *Parabacteroides*, which were also negatively correlated with the aforementioned pathways (green squares). These correlations were similar in the other comparisons with the control and BJC groups (Supplementary Fig. 3).

In contrast, sulfur metabolism, naphthalene, chloroalkene, and aminobenzoate degradation were exclusively relevant for HFD + BJC compared to HFD (Fig. 6). Furthermore, pathways related to lipid accumulation, including the citrate cycle, steroid hormone biosynthesis, lysosome, polyketide sugar unit biosynthesis, and atherosclerosis, were identified as relevant in HFD, further linking HFD to increased lipid accumulation and metabolic dysfunction [34]. These modulations indicate that BJC may influence carbohydrates and lipid metabolism in MetS through microbiota modulation.

Additionally, the identification of pathways involved in ferroptosis, streptomycin biosynthesis, and biofilm formation suggests that gut microbiota in the HFD group may adapt to a lipid-rich environment through the synthesis of antibiotics and biofilm formation as possible mechanisms for the damaged barrier function and reducing intestinal permeability by gut colonization of microbiota associated with MetS, potentially exacerbating MetS symptoms [34]. For the BJC group valine, leucine, and isoleucine degradation, two – component systems and lipopolysaccharide biosynthesis pathways were relevant. In the comparison of the HFD + BJC group with the control group (Suppl. Figure 3), the relevant pathways included fatty acid degradation, thiamine metabolism, MAPK signaling, glycolysis/gluconeogenesis, seleno-compound metabolism, phosphor-transferase system, fructose, and mannose metabolism.

These findings suggest that BJC administration revealed significant differences in metabolic pathway activation between the groups, highlighting its potential modulatory effect on MetS. Furthermore, the diversity of pathways associated with the microbiota abundances in the different evaluated treatments, such as amino acid degradation, two-component systems, and MAPK signaling, opens exciting possibilities. These pathways are key to understanding the profound alterations in microbiota that occur after BJC administration in normal and HFD conditions and their impact on metabolic parameters. These findings suggest that the relationship between BJC and dysbiosis-MetS is potentially complex, and further studies are needed to investigate the effects of BJC on the gut microbiome or individual bacteria.

1. **Microbial composition, metabolic pathways, and microbiota functions modulated by BJC and their correlation with biochemical parameters in the MetS model**

A comprehensive approach was employed to predict the functions and cellular pathways of relevant genera. Biochemical data such as weight or serum TC levels were used to perform correlation analyses, identifying 19 genera, 48 cellular pathways, and 83 functions with significant associations regardless of the treatment and diet (Figs. 7 and 8, and Supplementary Figs. 4 and 5, and Supplementary Tables 3 and 4).

The diversity of pathways associated with the microbiota abundances in the different evaluated treatments and their impact on metabolic parameters, such as amino acid degradation, two-component systems, and MAPK signaling, opens exciting possibilities. Several key associations emerged when focusing on the HFD + BJC group versus HFD alone, as shown in Fig. 7. The genus *Bifidobacterium* was positively correlated with body weight (ρ = 0.52, p = 0.02) and serum triglycerides (ρ = 0.51, p = 0.02), whereas *Akkermansia* abundance was positively correlated with serum TC (ρ = 0.58, p = 0.008). In contrast, *both Romboutsia* and *Adlercreutzia* were negatively correlated with serum AST levels (ρ = − 0.46, p = 0.04; ρ = − 0.55, p = 0.014, respectively). These findings suggest that the relationship between BJC and dysbiosis-MetS is potentially complex, and further studies are needed to investigate the effects of BJC on the gut microbiome or individual bacteria. The correlation analysis between the abundance of genera and biochemical markers underscores the intricate relationship between gut microbiota and metabolic health.

Additional significant relationships were observed across all treatments and dietary patterns. *Bifidobacterium*, the genus with the greatest number of associations, was also positively correlated with serum leptin (ρ = 0.56, *p*-val. = 0.013), total hepatic fat percentage (ρ = 0.62, *p*-val. = 0.004), and serum creatinine (ρ = 0.57, *p*-val. = 0.01), suggest that this genus plays a key role in metabolic deregulation. High fecal *Bifidobacterium* levels have been associated with overweight and obesity in children [35]. This highlights the potential of further research on this genus to advance targeted studies on MetS. While *Weissella* abundance was positively correlated with serum leptin (ρ = 0.47, *p*-val. = 0.038) and total hepatic fat percentage (ρ = 0.48, *p*-val. < 0.03), see Supplementary Fig. 4.

In contrast, *Allobaculum*, *Adlercreutzia*, *Clostridium sensu stricto 1*, and *Romboutsia* were all negatively associated with AST (ρ= -0.49, -0.46, -0.52, and − 0.55; *p*-val. = 0.03, 0.04, 0.02, and 0.014, respectively)

and with serum ALT levels ρ= -0.5, -0.41, -0.43, -0.56; *p*-val. = 0.07, 0.02, 0.06, and 0.01, respectively. These four genera, as well as *Turicibacter*, *Faecalibaculum*, *Ligilactobacillus*, and *Intestinimonas*, were positively associated with serum creatinine (ρ = 0.44–0.61, all *p*-val. < 0.05). Finally, *Lactoacillus* inversely correlates with AST (ρ= -0.5 and, *p*-val. = 0.015) *Saccharomyces cerevisiae* correlated positively with serum leptin (ρ = 0.49, *p*-val. = 0.03), *Bacteroides* with ileum fat area percentage (ρ = 0.46, *p*-val. = 0.04), *Parabacteroides* inversely correlated with serum leptin (ρ = − 0.48, *p*-val. = 0.03), and *Caproiciproducens* positively correlated with serum total cholesterol (ρ = 0.47, *p*-val. = 0.04) (Supplementary Tables 3 and 4). The other relevant genera were *Akkermansia* and *Bacteroidetes.* These were associated with serum TC levels and the ileum intestinal fat area percentage, respectively. Both phyla have been associated with the producting of short-chain fatty acids [36], which promote adipocyte leptin secretion, insulin sensitivity, and intestinal epithelium metabolism, and inhibit pathogenic bacteria. They also have anti-inflammatory actions, which underscores their potential as probiotics for MetS [34].

Parabacteroides and *Bacteroides* were relevant for the HFD + BJC and were associated with fatty acid biosynthesis and total ileum fat percentage. These were related to the phospholipid/cholesterol/gamma − HCH transport system ATP − binding protein, which participates in polyunsaturated fatty acid biosynthesis. Microbiota's polyunsaturated fatty acids can confer host resistance to obesity by reducing triacylglycerol accumulation [36]. In addition, other proteins, such as a magnesium transporter and gluconate 5-dehydrogenase, were negatively associated with fasting plasma glucose and may be related to changes in microbiota abundances that could lead to dysbiosis if these changes persist. For instance, magnesium deficiency modulates the abundance of gut *Bifidobacteria* and metabolic disorders in mice [37], whereas gluconate 5-dehydrogenase is necessary for bacterial growth and colonization of the large intestine, and it has been proposed as a target in bacterial infections. Another enzyme that was positively associated with *Parabacteroides* and *Bacteroides* is the alpha-L-rhamnosidase. This enzyme had a negative correlation with serum TC and insulin levels, both of which are related to MetS. BJC administration likely promotes the proliferation of *Parabacteroides*, impacting MetS by modulating short-chain and polyunsaturated fatty acids and steroid hormone biosynthesis, as well as producing α-L-rhamnosidase for the bioavailability of flavonoids [9] that have been linked to systemic and intestinal health [10], and potentially can participate in the reduction of high levels of serum TC and insulin, as is negatively correlated with these. Furthermore, the presence of α-L-rhamnosidase in the genomes of *Parabacteroides* and *Bacteroides* genera, as previously reported [38], indicates that this enzyme participates in the catabolism of berry cactus flavonoids and stimulates the utilization of L-rhamnose in berry cactus glycosides. Once L-rhamnose is free, it is metabolized to other carbohydrates, which can be used as a substrate throughout the fructose and mannose pathway and redirected to glycolysis or amino sugar and nucleotide sugar metabolism. The fructose and mannose pathways were correlated with fasting plasma glucose, creatinine, BUN, and the total ileum fat percentage. These findings emphasize the complex interactions between gut microbiota, metabolic pathways, and host biochemistry, revealing potential microbial targets for MetS therapeutic interventions. To develop effective strategies for combating MetS, future studies should focus on elucidating the molecular mechanisms by which BJC and other dietary interventions modulate MAB-associated metabolic functions.

Finally, the genomes of various genera were annotated to confirm the presence of genes in pathways correlated with the biochemical parameters assessed. A complex participation of all genera in the pathways was identified. As shown in Fig. 8, the dendrogram on the left side of the heatmap highlights the three main groups of functions correlated with the biochemical data (column dendrogram). At the bottom of the heat map, the first group was positively correlated with total ileum fat percentage and negatively correlated with serum leptin. The genera associated with these metabolic parameters include *Parabacteroides* and *Bacteroides* (Fig. 7-bottom of the heatmap), and these genera are relevant for the HFD + BJC group (Fig. 6). Besides, the metabolic pathways related to this group include the citrate cycle, fatty acid metabolism and biosynthesis, phenylalanine, tyrosine, and tryptophan biosynthesis, carbon metabolism, ubiquinone, and terpenoid-quinone biosynthesis, oxidative phosphorylation porphyrin and chlorophyll metabolism, and bacterial chemotaxis. Notably, the total ileum fat percentage was associated with the phospholipid/cholesterol/gamma − HCH transport system ATP − binding protein (ρ = 0.5, *p*-val. = 0.03), which participates in the biosynthesis of polyunsaturated fatty acids; perosamine synthetase (ρ = 0.47, *p*-val < 0.04), which synthesizes membrane lipopolysaccharides of Gram-negative bacteria; and alpha − L−rhamnosidase ρ = 0.46, *p*-val. = 0.05). Alpha − L−rhamnosidase was correlated inversely with leptin (ρ= -0.43, *p*-val. = 0.06) (Supplementary Fig. 5). These enzymes are negatively correlated with serum TC and insulin levels, both of which are related to MetS.

The center of the dendrogram (Fig. 8) shows the second group that negatively correlates with the total ileum fat percentage and BUN levels and is positive with serum TC, AST, ALT, and insulin levels. Genera such as *C. Saccharimonas*, *Akkermansia, Clostridium sensu stricto* 1, and *Adlercreutzia* show similar associations (Fig. 7-top of the heatmap). These genera are relevant to the HFD (Fig. 6). Pathways included peptidoglycan biosynthesis (ρ= -0.76, *p*-val. = 0.0001), pyrimidine metabolism (ρ= -0.62, *p*-val. = 0.004), among other related pathways (*p*-val. < 0.05) to amino acid biosynthesis, antibiotic resistance, and virulence factors (Fig. 5). Supplementary Table 4 shows the complete list of pathways, Spearman's coefficients, and p values. Serum TC levels were positively correlated (*p*-val. < 0.05) to the biosynthesis of amino acids (ρ = 0.48), lysine (ρ = 0.47), phenylalanine, tyrosine and tryptophan biosynthesis (ρ = 0.52), novobiocin biosynthesis (ρ = 0.47, *p*-val. = 0.04) and negatively associated with propanoate metabolism (ρ= -0.5, *p*-val. = 0.03). Serum insulin levels were positively correlated with glycerolipid metabolism (ρ = 0.46, *p*-val. = 0.04) (Fig. 8-middle of the heatmap). The functions related to the total ileum fat percentage were Xaa − Pro dipeptidase (ρ= -0.48, *p*-val. = 0.03), energy − coupling factor transport system *permease* protein (ρ= -0.48, *p*-val. = 0.04), oligopeptide transport system substrate − binding protein (ρ= -0.48, *p*-val. = 0.04), thioredoxin reductase (NADPH) (ρ= -0.51, p-val. = 0.02), cysteine desulfurase (ρ= -0.54, *p*-val. = 0.016), and ATP − dependent Clp protease ATP − binding subunit ClpE (ρ= -0.54, *p*-val. = 0.016) (Supplementary Fig. 5).

On top of the heatmap (Fig. 8), the third group of functions is positively associated with fasting plasma glucose, creatinine, and BUN and negatively associated with serum AST and ALT levels (Fig. 8). *Clostridium sensu stricto 1*, Adlercreutzia, Allobaculum, Ligilactobacillus, *Faecalibacterium*, *Turicibacter*, and *Intestinimonas* have similar associations (Fig. 7-top of the heatmap). These genera were relevant for the control and BJC groups and irrelevant for HFD + BJC. The pathways included MAPK signaling (ρ =

0.63, *p*-val. = 0.003), glucagon signaling (ρ = 0.6, *p*-val. = 0.006), fructose and mannose metabolism (ρ = 0.59, *p*-val. = 0.008), hypoxia-inducible factor-1 signaling (ρ = 0.55, *p*-val. = 0.01), ascorbate and aldrete metabolism (ρ = 0.47, *p*-val. = 0.04), and amino and nucleotide sugar metabolism (ρ = 0.5, *p*-val. = 0.03). Moreover, functions that show a negative association with serum AST levels include the glucagon signaling pathway (ρ= -0.54, *p*-val. = 0.01), *S. aureus* infection (ρ= -0.48, *p*-val. = 0.03), starch and sucrose metabolism (ρ= -0.46, *p*-val. = 0.04), sulfur metabolism (ρ= -0.47, *p*-val. = 0.04), serum ALT (ρ= -0.54, *p* val. = 0.016; Fig. 7). Protein − tyrosine phosphatase was associated with glucose (ρ = 0.55, *p*-val. = 0.02) and serum creatinine levels (ρ = 0.65, *p*-value). < 0.01) and, as well as magnesium transporter, positively associated with serum creatinine (ρ = 0.6, *p*-val. < 0.002) and negatively correlated with serum AST (ρ= -0.49, *p*-val. = 0.03). Gluconate 5 − dehydrogenase had an inverse correlation with serum glucose (ρ= -0.62, *p*-val. = 0.005) and creatinine (ρ= -0.6, *p*-value = 0.06) (Supplementary Fig. 5).

Other metabolic parameters with significant associations included the percentage of total adipose tissue fat with *Oscillospira* (ρ = 0.52, *p*-val. = 0.02; Fig. 7-bottom of the heatmap), serum ALT with *Fusicatenibacter* (ρ = 0.48, *p*-val. = 0.038; Fig. 7-bottom of the heatmap), arginine biosynthesis (ρ = 0.49, *p*-val. = 0.03), oxidative phosphorylation (ρ = 0.55, *p*-val. = 0.013), and sulfur metabolism (ρ= −0.54, *p*-val. = 0.016). Serum creatinine with C5 − branched dibasic acid metabolism (ρ = 0.48, *p*-val. = 0.03), oxidative phosphorylation (ρ= -0.53, *p*-val. = 0.018), chromate transporter (ρ= -0.53, *p*-val. = 0.008), and beta galactosidase (ρ= -0.53, *p*-val. = 0.018). BUN levels were associated with a two − component system (ρ = 0.51, *p*-val. = 0.02), biofilm formation − *E. coli* (ρ = 0.64, *p*-val. = 0.003), and fructose and mannose metabolism (ρ = 0.59, *p*-val. = 0.008) (Fig. 8-bottom of the heatmap). In addition, BUN levels were associated with different families (OmpR, NarL, and NtrC) of two-component system sensor histidine kinases (*p*-val. < 0.01). Ammonium transporters in the Amt family were correlated with BUN (ρ = 0.67, *p*-val. = 0.001). However, specific genera promote the bioavailability of some carbohydrates. For example, all the mentioned genera contain fructose and mannose metabolism genes. However, as previously described, *Bacteroides* and *Parabacteroides* preferentially participate in the catabolism of glycosides containing terminal L-rhamnose present in berry cactus flavonoids.

4. Conclusions

The use of BJC is a promising source of biomolecules to improve metabolic conditions for patients with obesity, MetS, or with a high risk of MetS development, considering that BJC treatment prevents the increase of body weight, fasting plasma glucose, triglycerides, TC, and insulin. It also reduces fat accumulation in hepatic, intestinal, and adipose tissues. BJC modifies the diversity of microbiota, maintaining phyla abundances like those in the control groups. In this study, BJC administration in HFD rats induced dysbiosis that were linked to several pathways involved in maintaining energy homeostasis, including carbohydrates, amino acids, and lipid metabolism. Adequate regulation of these mechanisms is associated with reduced cardiovascular and obesity risks. It is suggested that compounds found in BJC or fresh fruit have a direct impact on microbiota diversity that may improve obesity, dyslipidemia, or MetS. BJC administration increased the *Parabacteroides* genus; this has been related to the transport and production of short-chain fatty acids metabolism and steroid hormones, as well as stimulating the

production of bioactive compounds by promoting the establishment of microbiota producing α-l-rhamnosidase that may improve the pro-inflammatory environment and reduce the intestinal leaking induced by HFD. However, the exact mechanism of action needs to be studied in detail.

Furthermore, complementary analyses, such as transcriptomics and metabolomics of the liver, intestine, kidney and adipose tissue, are necessary to investigate the host organs' response to BJC administration. In addition, the bioactive compounds in the berry cactus responsible for the effects observed here remain unidentified, and their characterization is essential to elucidate potential action mechanisms and to propose its use as an adjuvant in the treatment of MetS and other non-communicable diseases.

Declarations

Acknowledgments

The authors would like to thank the IIMx program-SECIHTI for supporting projects 615 (JT) and 809 (COV). COV would like to acknowledge the support of the IPICYT's National Supercomputing Center with the computational grant TKII- R2018-COV1. The SECIHTI played no role in the design, analysis, or writing of this article. We thank M.C. for technical support. Alberto Barrera (IPICYT), and Dr. Ricardo Espinosa-Tanguma (UASLP) for the facilities granted and the use of equipment, as well as the vivarium of the Faculty of Medicine (UASLP).

Ethical statement

This study was conducted according to the ARRIVE 2.0 guidelines for studies in animals.

Statement of authors' contributions

The authors' responsibilities were as follows – JT and COV: designed the research; JNGC, VR, CJB, MSP, YRR, NGH, AKRV, RW: conducted research; JNGC, VR, CJB, MSP, JT, COV: analyzed data; JNGC, VR, YRR, JT, COV: wrote the article; JT, COV, VR: had primary responsibility for final content; and all authors: read and approved the final manuscript.

Funding sources

The authors thank SECIHTI previously CONAHCYT for supporting this research with the FORDECYT-101732 grant. The postdoctoral and doctoral scholarship from SECIHTI previously CONAHCYT (FORDECYT-101732) supports JNGC, YRR and AKRV.

References

1. Mazidi M, Rezaie P, Kengne AP et al (2016) Gut microbiome and Metabolic Syndrome. Diabetes & Metabolic Syndrome: Clinical Research &. https://doi.org/10.1016/j.dsx.2016.01.024. Reviews 1–8

2. Aguilar M, Bhuket T, Torres S et al (2015) Prevalence of the metabolic syndrome in the United States, 2003–2012. JAMA 313:1973–1974. https://doi.org/10.1001/jama.2015.4260
3. Hajat C, Shather Z (2012) Prevalence of metabolic syndrome and prediction of diabetes using IDF versus ATPIII criteria in a Middle East population. Diabetes Res Clin Pract 98:481–486. https://doi.org/10.1016/j.diabres.2012.09.037
4. Gutiérrez-Solis AL, Datta Banik S, Méndez-González RM (2018) Prevalence of Metabolic Syndrome in Mexico: A Systematic Review and Meta-Analysis. Metab Syndr Relat Disord 16. https://doi.org/10.1089/met.2017.0157
5. Hazime H, Ducasa G, Brito N et al (2023) Loss of epithelial duox2 signaling is accompanied by a reduction in A*kkermansiaceae* and promotes the development of metabolic syndrome in a microbiome-dependent manner. Inflamm Bowel Dis 29. https://doi.org/10.1093/ibd/izac247.136
6. Arumugam M, Raes J, Pelletier E et al (2011) Enterotypes of the human gut microbiome. Nature 473. https://doi.org/10.1038/nature09944
7. Song Q, Cheng SW, Zou J et al (2024) Role of gut microbiota on regulation potential of Dendrobium officinale Kimura & Migo in metabolic syndrome: In-vitro fermentation screening and in-vivo verification in db/db mice. J Ethnopharmacol 321. https://doi.org/10.1016/j.jep.2023.117437
8. Sandoval-Salazar C, Jiménez-García SN, Beltrán-Campos V et al (2023) Effect of berrycactus fruit (Myrtillocactus geometrizans) on glutamate, glutamine, and GABA levels in the frontal cortex of rats fed with a high-fat diet. Open Life Sci 18. https://doi.org/10.1515/biol-2022-0529
9. Luo B, Wen Y, Ye F et al (2023) Bioactive phytochemicals and their potential roles in modulating gut microbiota. J Agric Food Res 12. https://doi.org/10.1016/j.jafr.2023.100583
10. Sánchez-Recillas E, Almanza-Aguilera E, Dufoo-Hurtado E et al (2024) Untargeted metabolomics of gut-derived metabolites from in vitro colonic fermentation of garambullo (Myrtillocactus geometrizans). J Funct Foods 114. https://doi.org/10.1016/j.jff.2024.106063
11. Ramírez-Rodríguez Y, Ramírez V, Robledo-Márquez K et al (2022) Stenocereus huastecorum-fruit juice concentrate protects against cisplatin-induced nephrotoxicity by nitric oxide pathway activity and antioxidant and antiapoptotic effects. Food Res Int 160:111337. https://doi.org/10.1016/j.foodres.2022.111337
12. Avila-Nava A, Noriega LG, Tovar AR et al (2017) Food combination based on a pre-hispanic Mexican diet decreases metabolic and cognitive abnormalities and gut microbiota dysbiosis caused by a sucrose-enriched high-fat diet in rats. Mol Nutr Food Res 61. https://doi.org/10.1002/mnfr.201501023
13. Ramírez-Rodríguez Y, Espinosa-Tanguma R, Valle-Aguilera JR et al (2024) Vasorelaxant Effect and Blood Pressure Reduction Potential of Pitaya Juice Concentrate (Stenocereus huastecorum) Associated with Calcium Channel Blockade. Foods 13. https://doi.org/10.3390/foods13162631
14. Trujillo J, Chirino Yolanda I, Martínez-Tagüeña N, Pedraza-Chaverri J (2018) Renal damage in the metabolic syndrome (MetSx): Disorders implicated. Eur J Pharmacol 818. https://doi.org/10.1016/j.ejphar.2017.11.032

15. Ramírez-Rodríguez Y, Martínez-Huélamo M, Pedraza-Chaverri J et al (2020) Ethnobotanical, nutritional and medicinal properties of Mexican drylands Cactaceae Fruits: Recent findings and research opportunities. Food Chem
16. Duarte-Alonso A, Cu-Cañetas TE, Avila-Nava A et al (2020) A Cecropia peltata ethanolic extract reduces insulin resistance and hepatic steatosis in rats fed a high-fat diet. J Ethnopharmacol 261. https://doi.org/10.1016/j.jep.2020.113087
17. Haro C, Garcia-Carpintero S, Alcala-Diaz JF et al (2016) The gut microbial community in metabolic syndrome patients is modified by diet. J Nutr Biochem 27. https://doi.org/10.1016/j.jnutbio.2015.08.011
18. Huang Y, Cao J, Zhu M et al (2024) Bacteroides fragilis aggravates high-fat diet-induced non-alcoholic fatty liver disease by regulating lipid metabolism and remodeling gut microbiota. Microbiol Spectr 12. https://doi.org/10.1128/spectrum.03393-23
19. Jin H, Zhang C (2020) High fat high calories diet (HFD) increase gut susceptibility to carcinogens by altering the gut microbial community. J Cancer 11:4091–4098. https://doi.org/10.7150/jca.43561
20. Burger O, Ofek I, Tabak M et al (2000) A high molecular mass constituent of cranberry juice inhibits Helicobacter pylori adhesion to human gastric mucus. FEMS Immunol Med Microbiol 29. https://doi.org/10.1016/S0928-8244(00)00220-0
21. Xie Y, Pei F, Liu Y et al (2023) Fecal fermentation and high-fat diet-induced obesity mouse model confirmed exopolysaccharide from Weissella cibaria PFY06 can ameliorate obesity by regulating the gut microbiota. Carbohydr Polym. https://doi.org/10.1016/j.carbpol.2023.121122. 318:
22. Zhao L, Shen Y, Wang Y et al (2022) Lactobacillus plantarum S9 alleviates lipid profile, insulin resistance, and inflammation in high-fat diet-induced metabolic syndrome rats. Sci Rep 12. https://doi.org/10.1038/s41598-022-19839-5
23. Medina-Larqué AS, Rodríguez-Daza MC, Roquim M et al (2022) Cranberry polyphenols and agave agavins impact gut immune response and microbiota composition while improving gut barrier function, inflammation, and glucose metabolism in mice fed an obesogenic diet. Front Immunol 13. https://doi.org/10.3389/fimmu.2022.871080
24. An HM, Park SY, Lee DK et al (2011) Antiobesity and lipid-lowering effects of Bifidobacterium spp. in high fat diet-induced obese rats. Lipids Health Dis 10. https://doi.org/10.1186/1476-511X-10-116
25. Skrovankova S, Sumczynski D, Mlcek J et al (2015) Bioactive compounds and antioxidant activity in different types of berries. Int J Mol Sci 16
26. Milton-Laskibar I, Marcos-Zambrano LJ, Gómez-Zorita S et al (2022) Involvement of microbiota and short-chain fatty acids on non-alcoholic steatohepatitis when induced by feeding a hypercaloric diet rich in saturated fat and fructose. https://doi.org/10.1017/gmb.2022.2. Gut Microbiome 3:
27. Jiao X, Wang Y, Lin Y et al (2019) Blueberry polyphenols extract as a potential prebiotic with anti-obesity effects on C57BL/6 J mice by modulating the gut microbiota. J Nutr Biochem. https://doi.org/10.1016/j.jnutbio.2018.07.008. 64:

28. Lessard-Lord J, Roussel C, Lupien-Meilleur J et al (2024) Short term supplementation with cranberry extract modulates gut microbiota in human and displays a bifidogenic effect. NPJ Biofilms Microbiomes 10. https://doi.org/10.1038/s41522-024-00493-w
29. Espín JC, Jarrín-Orozco MP, Osuna-Galisteo L et al (2024) Perspective on the Coevolutionary Role of Host and Gut Microbiota in Polyphenol Health Effects: Metabotypes and Precision Health. Mol Nutr Food Res 68
30. Yu DY, Kim SH, Kim JA et al (2018) Effects of Rubus coreanus byproducts on intestinal microbiota and the immune modulation. Asian-Australas J Anim Sci 31. https://doi.org/10.5713/ajas.17.0733
31. Rodríguez-Daza MC, Daoust L, Boutkrabt L et al (2020) Wild blueberry proanthocyanidins shape distinct gut microbiota profile and influence glucose homeostasis and intestinal phenotypes in high-fat high-sucrose fed mice. Sci Rep 10. https://doi.org/10.1038/s41598-020-58863-1
32. Chansa O, Shantavasinkul PC, Monsuwan W, Sirivarasai J (2024) Association between Gut Microbiota Profiles, Dietary Intake, and Inflammatory Markers in Overweight and Obese Women. Foods 13. https://doi.org/10.3390/foods13162592
33. Lin H, An Y, Hao F et al (2016) Correlations of Fecal Metabonomic and Microbiomic Changes Induced by High-fat Diet in the Pre-Obesity State. Sci Rep 6. https://doi.org/10.1038/srep21618
34. Duan X, Zhang L, Liao Y et al (2024) Semaglutide alleviates gut microbiota dysbiosis induced by a high-fat diet. Eur J Pharmacol 969. https://doi.org/10.1016/j.ejphar.2024.176440
35. Da Silva CC, Monteil MA, Davis EM (2020) Overweight and Obesity in Children Are Associated with an Abundance of Firmicutes and Reduction of Bifidobacterium in Their Gastrointestinal Microbiota. https://doi.org/10.1089/chi.2019.0280. Childhood Obesity 16:
36. Sanna S, van Zuydam NR, Mahajan A et al (2019) Causal relationships among the gut microbiome, short-chain fatty acids and metabolic diseases. Nat Genet 51
37. Pachikian BD, Neyrinck AM, Deldicque L et al (2010) Changes in intestinal bifidobacteria levels are associated with the inflammatory response in magnesium-deficient mice. J Nutr 140. https://doi.org/10.3945/jn.109.117374
38. Wu T, Pei J, Ge L et al (2018) Characterization of a α-L-rhamnosidase from Bacteroides thetaiotaomicron with high catalytic efficiency of epimedin C. Bioorg Chem 81. https://doi.org/10.1016/j.bioorg.2018.08.004

Figures

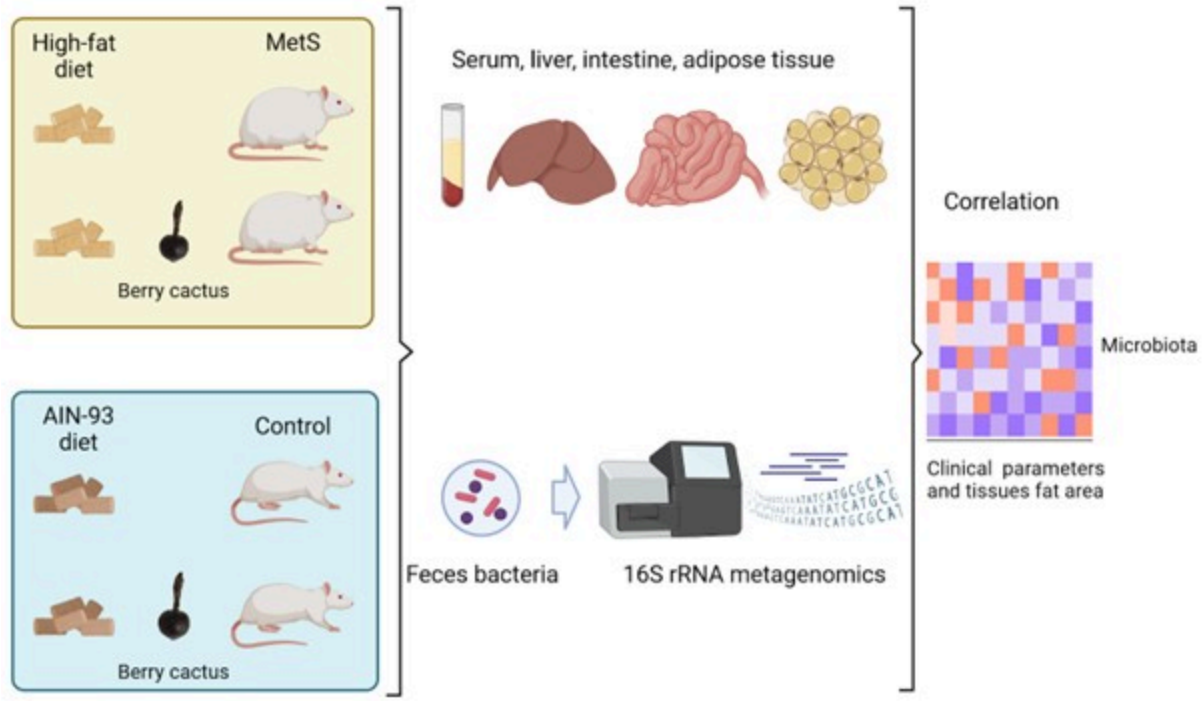

Figure 1

Experimental design. Four groups of rats (n = 5) were included in the experiment. The control group was fed the AIN 93 diet. The BJC group was fed with the AIN 93 diet, plus BJC was administered (blue box). The HFD group was fed 45% calories from lipids based on lard. The HFD + BJC group was fed a 45% HFD and administered BJC (yellow box). After 140 days, plasma, the subcutaneous adipose tissue, the right inferior lobule of the liver, and the intestine of each animal were obtained. Biochemical markers, including glucose, triglycerides, total cholesterol (TC), alanine aminotransferase (ALT), aspartate aminotransferase (AST), creatinine, insulin, and blood urea nitrogen (BUN) levels, were assessed in plasma. 16S rRNA metagenomic data from the fresh feces samplers of the animals were obtained. Biochemical parameters were correlated with microbiota abundance data. The Figure was created using BioRender.com.

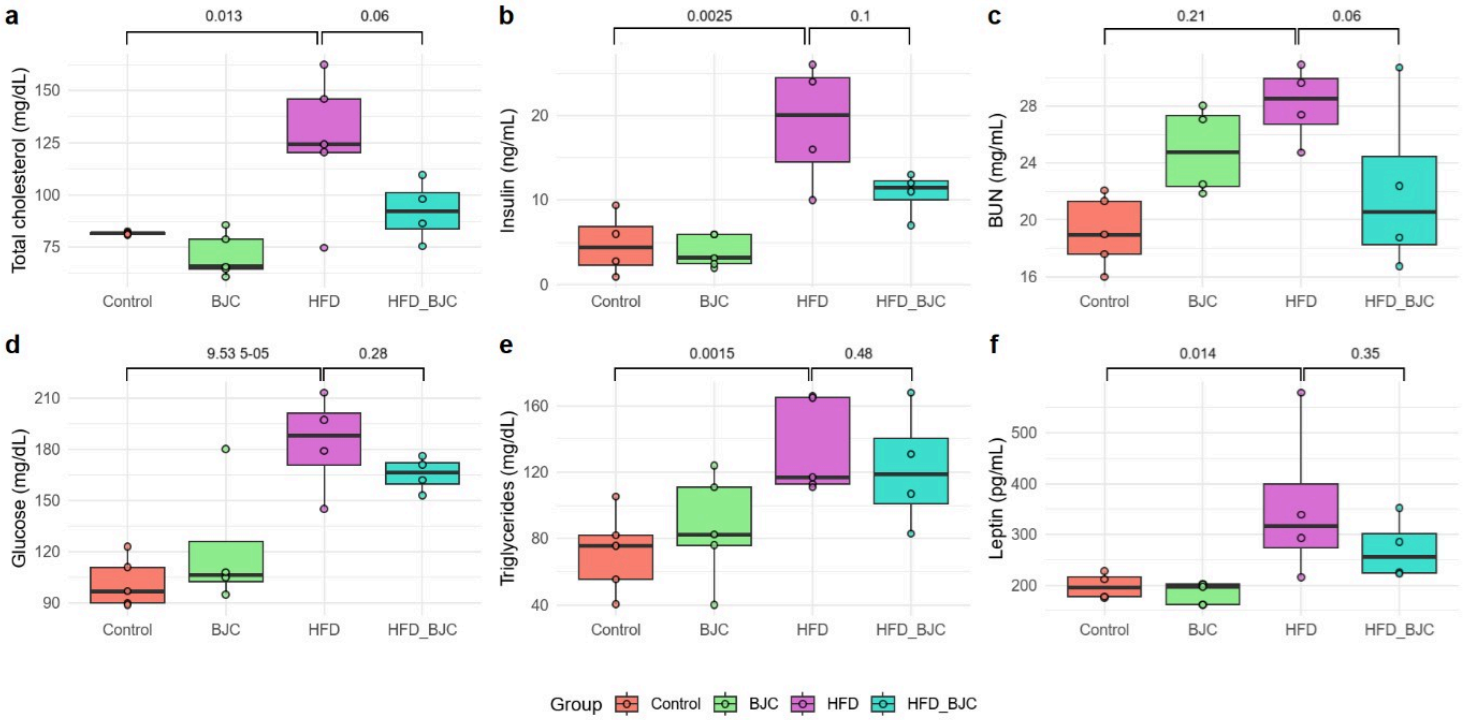

Figure 2

Noteworthy biochemical parameters in rats with MetS. (a) Glucose, (b) triglycerides, (c) total cholesterol, (d) leptin, (e) insulin, and (f) blood urea nitrogen (BUN). Control, AIN-93 diet control group. BJC (200 mg/kg), AIN-93 diet plus BJC treatment group. HFD, high-fat diet group (45%). HFD-BJC, high-fat diet with BJC treatment. The comparison's p-value is shown over the comparison line. Significant differences in biochemical parameters were considered with a *p*-val. < 0.05 (Welch's t-test). n = 5.

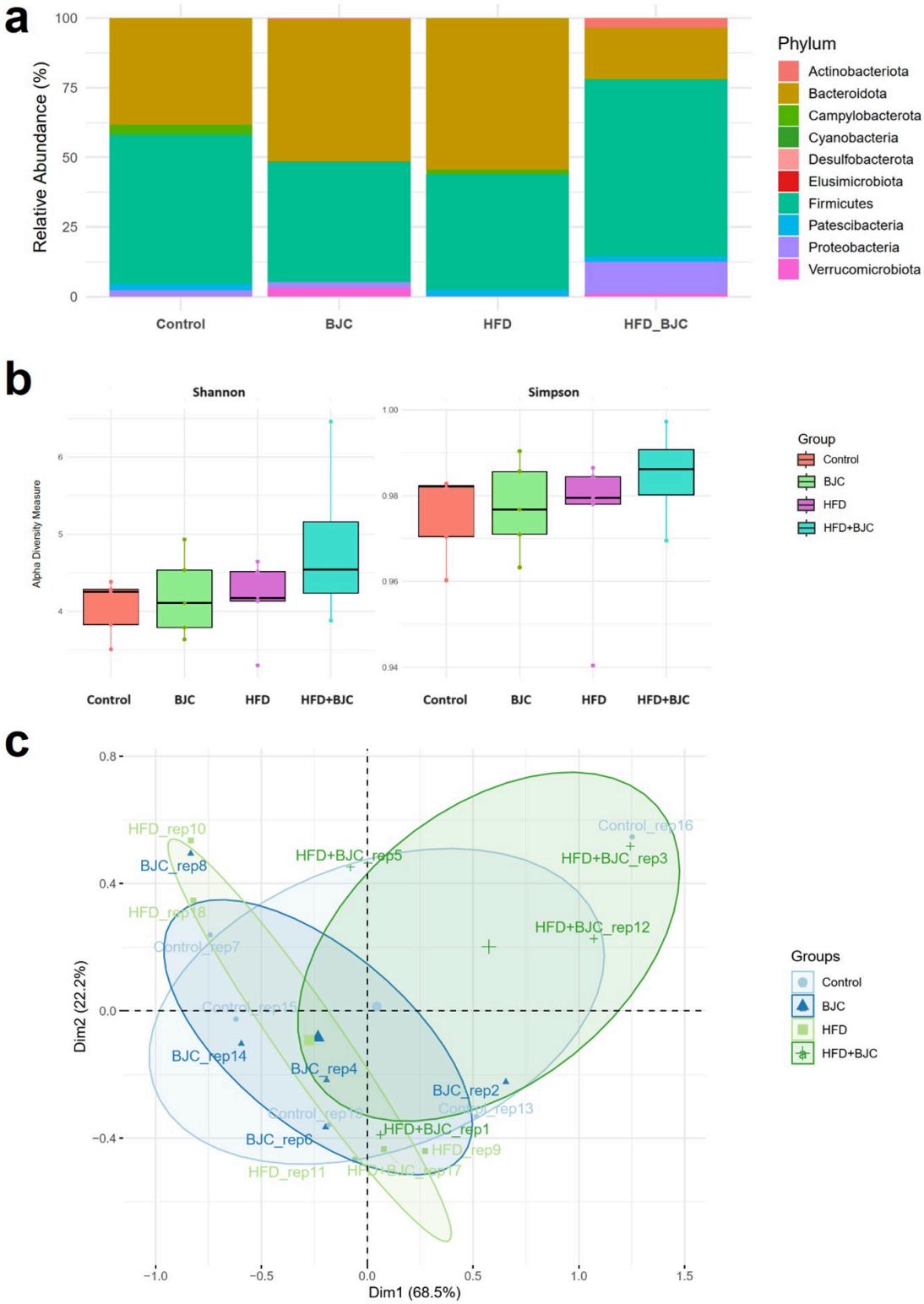

Figure 3

Diversity and relative abundances at the phylum level of the experimental groups. (a) Phylum relative abundance in experimental groups. (b) Shannon and Simpson alpha diversity distributions. (c) Principal Coordinates Analysis (PCA) using relative abundance data to show the beta diversity of the groups.

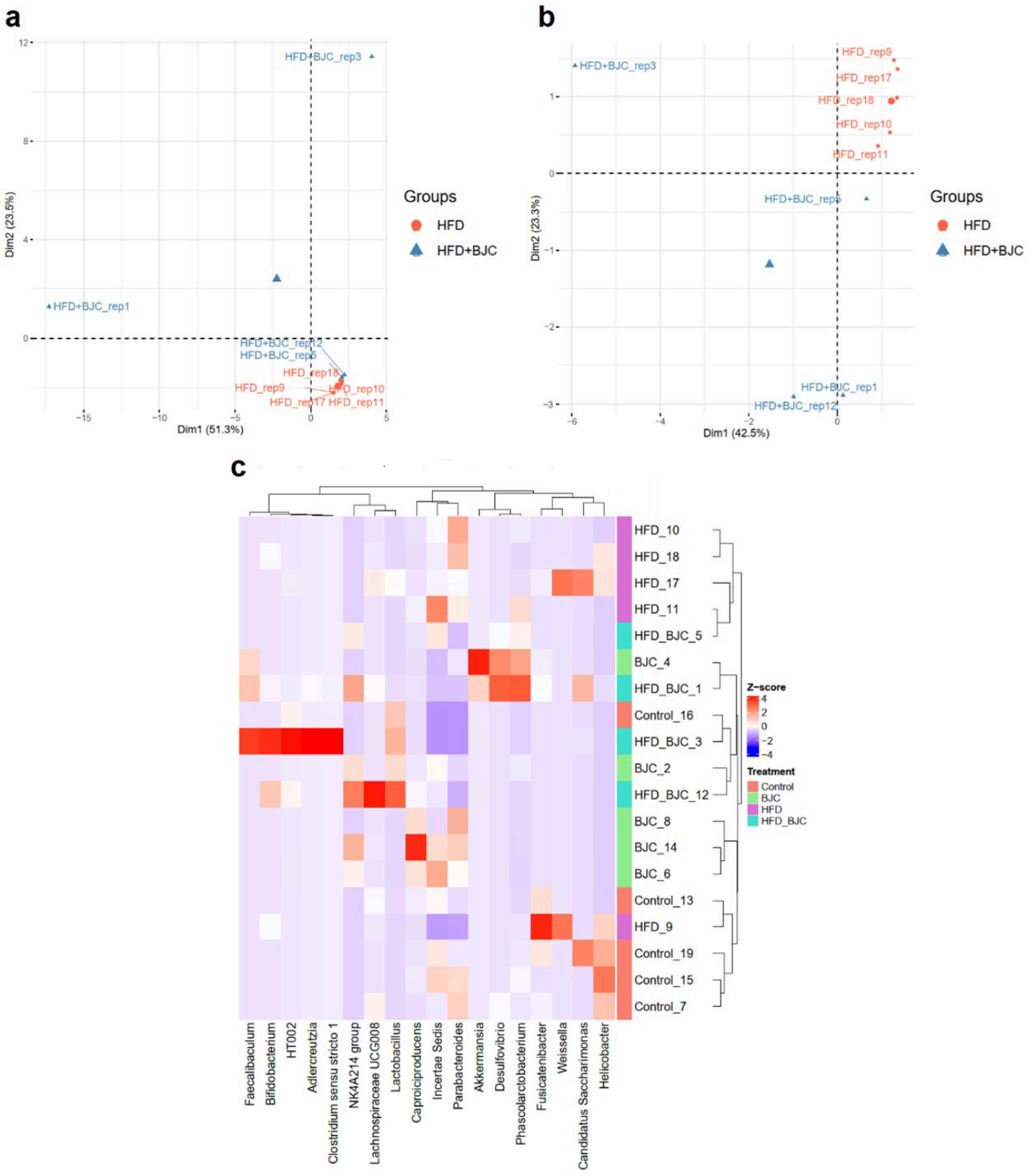

Figure 4

sPLS-DA identifies relevant differences in microbiota in the experimental groups. (a) Biplot using all genera in the HFD and HFD + BJC contrast groups. (b) PCoA using all genera in the HFD and HFD + BJC contrast. (c) Heatmap showing the Z-scores of the relevant genera associated with the treatments. The dendrogram on the right of the heatmap shows the samples. Control, AIN-93 diet control group (red).

BJC, AIN-93 diet plus BJC treatment group (green). HFD, high-fat diet group (purple). HFD-BJC, high-fat diet with CC treatment (cyan).

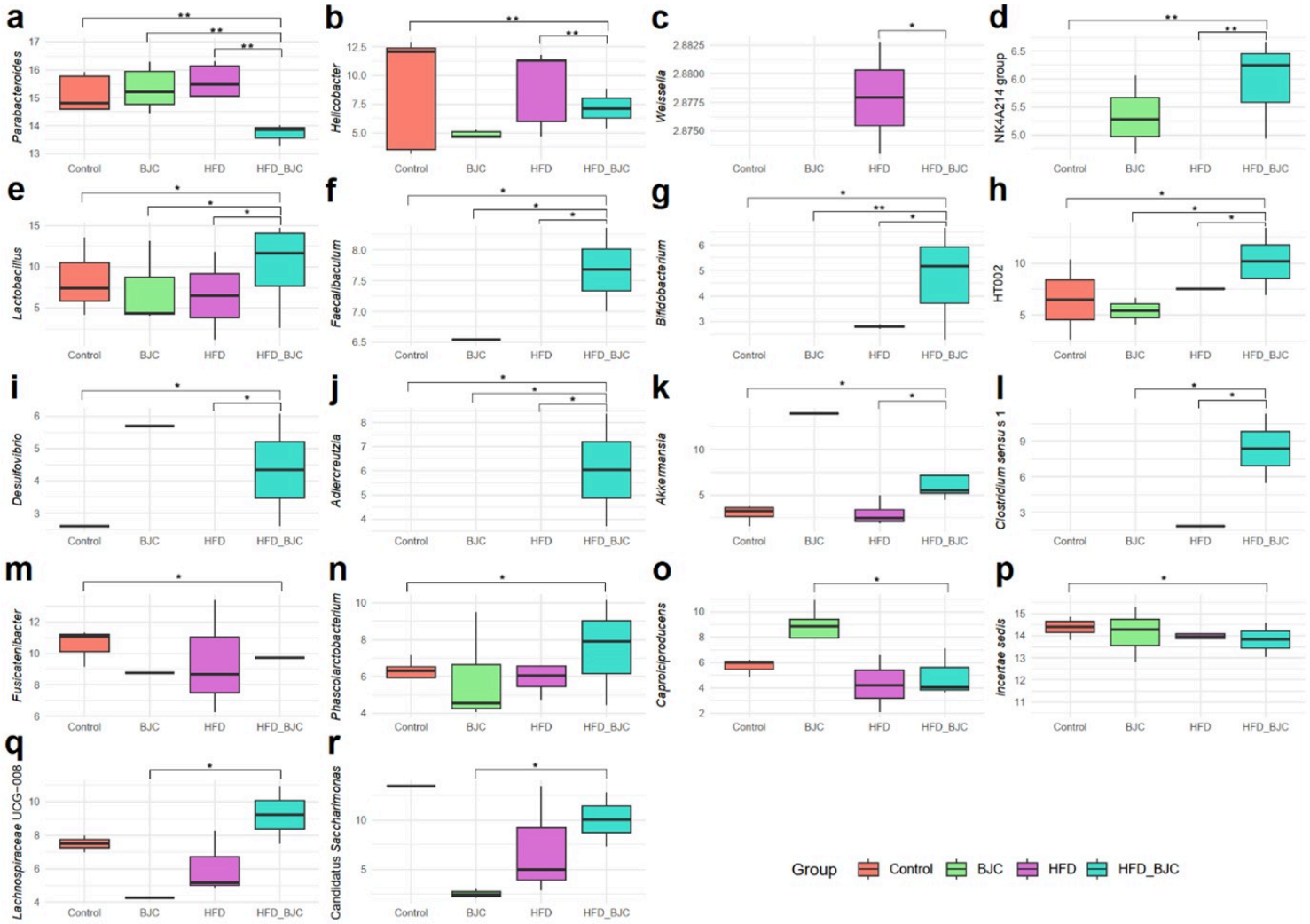

Figure 5

Boxplots showing the abundance observed in relevant genera associated with the treatments. (a) *Parabacteroides*. (b) *Helicobacter*. (c) *Weisella*. (d) NK4A214 group. (e) *Lactobacillus*. (f) *Faecalibaculum*. (g) *Bifidobacterium*. (h) HT0002. (i) *Desulfovibrio*. (j)*Adlercreutzia*. (k) *Akkermansia*. (l) *Clostridium sensu stricto* 1. (m) *Fusicatenibacter*. (n) *Phascolarctobacterium*. (o) *Caproiciproducens*. (p) *Incertae sedis*. (q) *Lachnospiraceae* UCG-008. (r) Candidatus *saccharimonas*. The significance of the comparison (sPLS-DA permutation test) is shown with asterisks: *, *p*-val. < 0.1 >0.01; ** *p*-val < 0.01. Control, AIN-93 diet control group (red). BJC, AIN-93 diet plus BJC treatment group (green). HFD, high-fat diet group (purple). HFD-BJC, high-fat diet with CC treatment (cyan).

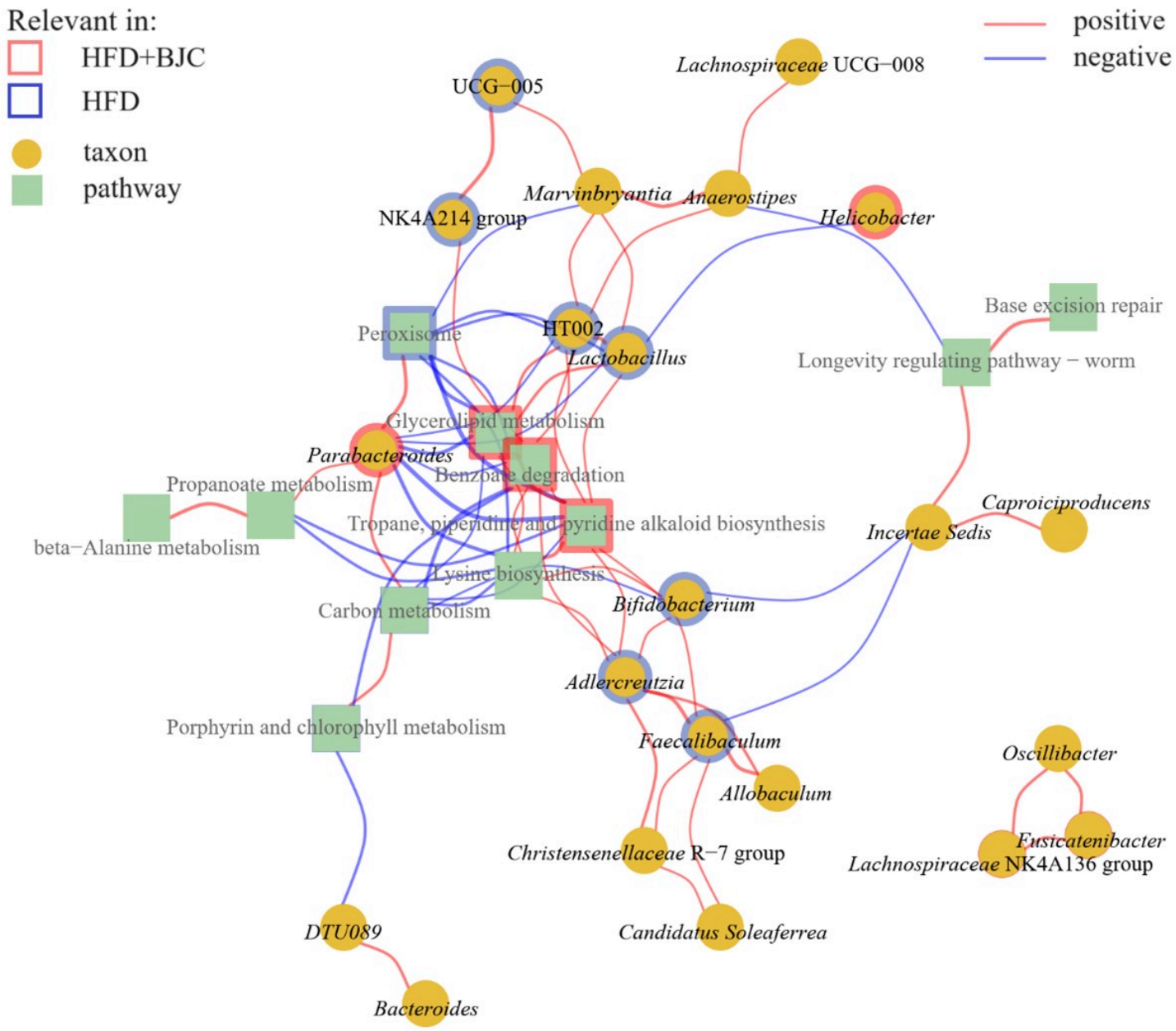

Figure 6

Association between genus abundance and pathways. The relevant genus and pathway nodes are indicated by yellow circles and green squares, respectively. The red and blue lines indicate the positive and negative Spearman correlations, respectively.

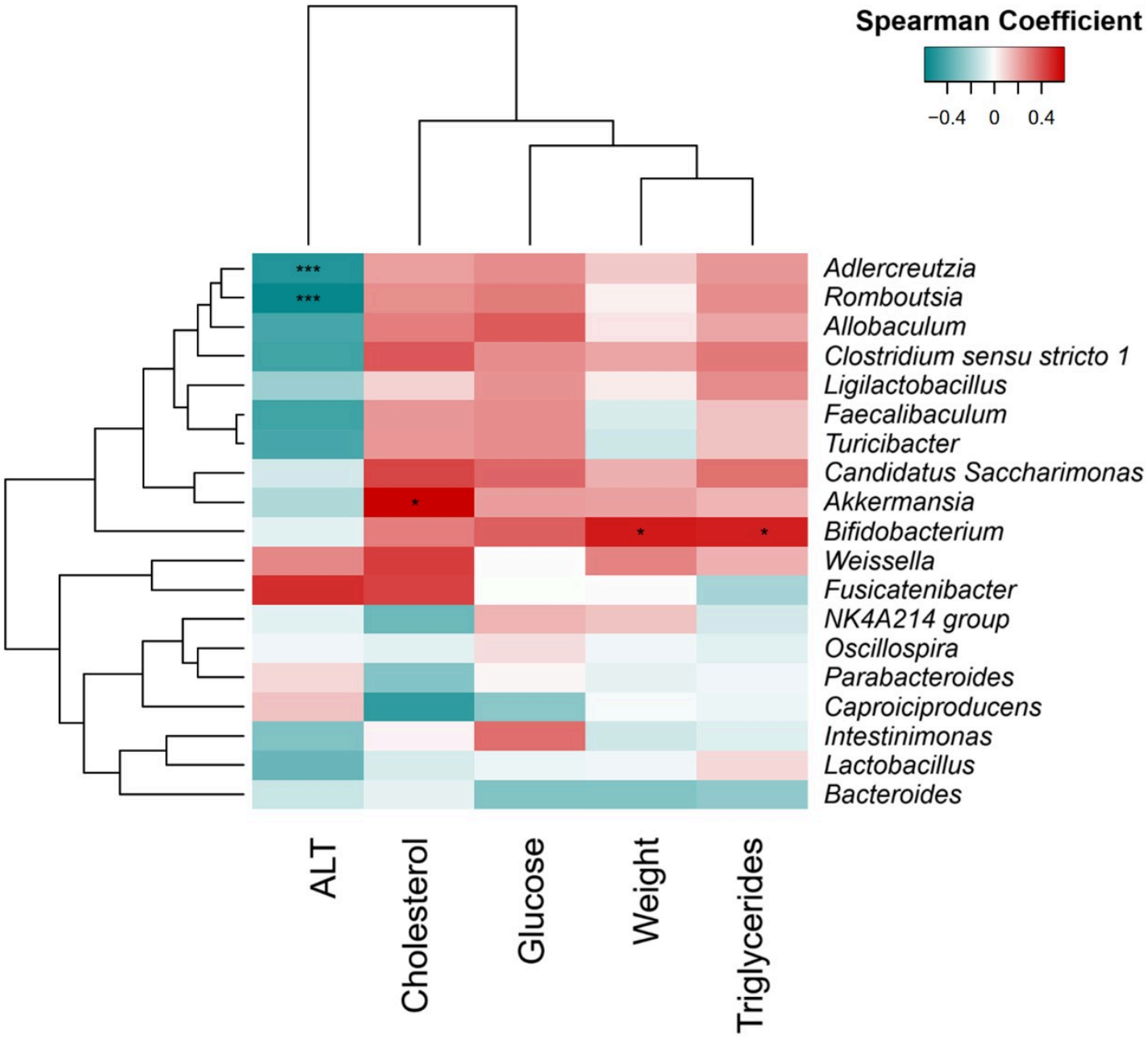

Figure 7

Correlations between genus abundance and biochemical parameters Positive and negative Spearman coefficients are shown in red and blue, respectively. Only Spearman correlation coefficients > |0.3| and *p*-value < 0.1 are shown. (*) *p*-value <0.05; (**) *p*-value < 0.01

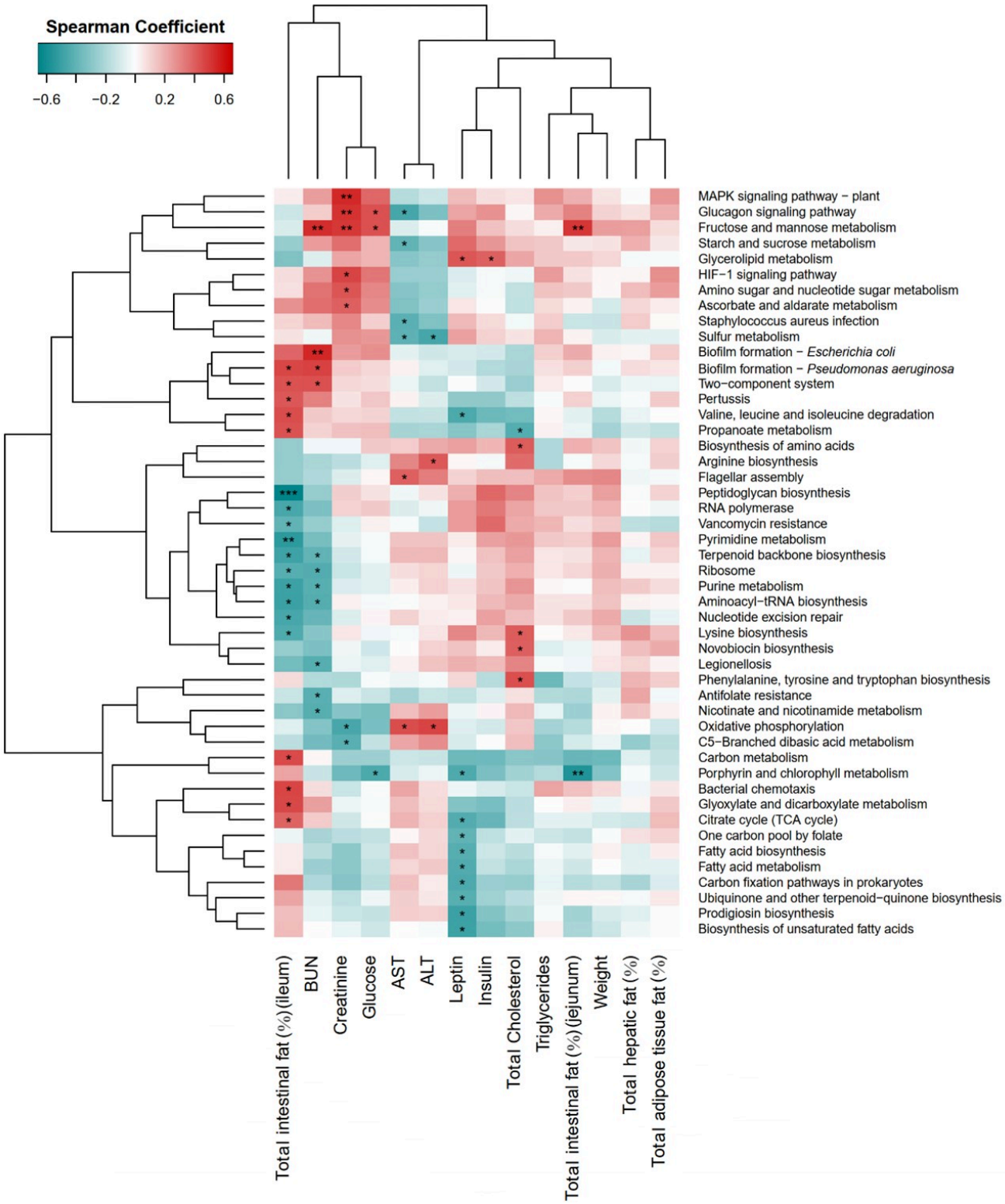

Figure 8

Spearman correlations between pathways and biochemical parameters Positive Spearman correlation coefficients are shown in red, and negative correlation coefficients are shown in blue. Only Spearman correlation coefficients > |0.3| and *p*-value < 0.1 are shown. **p*-value <0.05; ***p*-value < 0.01.

Supplementary Files

This is a list of supplementary files associated with this preprint. Click to download.

- SupplementaryTableS3.Biochemicalparametersgeneraabundancespathwaysandfunctionsdata.csv
- SupplementaryTableS4.Spearmancoefficientsandpvaluesofbiochemicalparameterscorrelations.csv
- Supplementary.docx